ISSN 0006-2979, Biochemistry (Moscow), 2006, Vol. 71, No. 9, pp. 1021-1026. © Pleiades Publishing, Inc., 2006.
Original Russian Text © M. V. Kozlov, K. M. Polyakov, A. V. Ivanov, S. E. Filippova, A. O. Kuzyakin, V. L. Tunitskaya, S. N. Kochetkov, 2006, published in Biokhimiya, 2006, Vol. 71, No. 9, pp. 1253-1259.
Originally published in Biochemistry (Moscow) On-Line Papers in Press, as Manuscript BM06-072, June 11, 2006.

Hepatitis C Virus RNA-Dependent RNA Polymerase: Study on the Inhibition Mechanism by Pyrogallol Derivatives

M. V. Kozlov*, K. M. Polyakov, A. V. Ivanov, S. E. Filippova, A. O. Kuzyakin, V. L. Tunitskaya, and S. N. Kochetkov

Engelhardt Institute of Molecular Biology, Russian Academy of Sciences, ul. Vavilova 32, 119991 Moscow, Russia; fax: (495) 135-1405; E-mail: kozlovmv@hotmail.com

Received March 22, 2006
Revision received March 29, 2006

Abstract—Pyrogallol reversibly and noncompetitively inhibits the activity of the hepatitis C RNA-dependent RNA polymerase. Based on molecular modeling of the inhibitor binding in the active site of the enzyme, the inhibition was suggested to be realized via chelation of two magnesium cations involved in the catalysis at the stage of the phosphoryl residue transfer. The proposed model allowed us to purposefully synthesize new derivatives with higher inhibitory capacity.

DOI: 10.1134/S0006297906090112

Key words: hepatitis C virus, RNA-dependent RNA polymerase, pyrogallol derivatives, inhibition mechanism, molecular modeling

The hepatitis C virus (HCV) is one of the most world-wide distributed human pathogens. At present, about 3% of the world's population (170 millions) are infected with HCV [1, 2]. In many infected persons, liver cirrhosis develops within about 20 years, which can subsequently lead to hepatocellular carcinoma [3]. The current treatment for hepatitis C is virtually founded only on interferon α and its combination with the nucleoside analog ribavirin [4]. But the efficiency of this therapy is very low, especially in the case of the first genotype virus, which is the most common in Russia (less than 30% of the patients are sensitive to the treatment).

The HCV RNA-dependent RNA polymerase (RdRp, the viral protein NS5B) seems to be a promising target for new approaches to the treatment of hepatitis C, because normally the liver cell contains no proteins with a similar activity. The HCV RdRp, which is the main component of the HCV replicative complex, is a protein with molecular weight of about 70 kD and is structurally related to other viral and bacterial RNA and DNA single-subunit polymerases [5]. The RdRp inhibitors reported so far can be conventionally subdivided into two main classes: nucleoside derivatives and various non-nucleoside inhibitors [6, 7]. Among the non-nucleoside inhibitors, derivatives of α,γ-diketo acids, in particular, 2,4-dioxo-4-phenylbutanoic acid (DKA), are of special interest (Fig. 1a).

The structure of DKA is specified by a coplanar location of three oxygen-containing functional groups conjugated with the aromatic fragment of the molecule. These groups are supposed to chelate Mg^{2+} which are present in the active site of HCV RdRp and other RNA and DNA

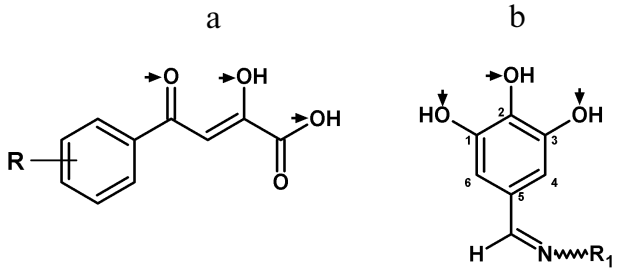

Fig. 1. General formulas of DKA derivatives (a) and the synthesized 5-substituted pyrogallol derivatives (b). The arrows indicate the oxygen-containing ligands.

Abbreviations: DKA) 2,4-dioxo-4-phenylbutanoic acid; CN-DKA) 4-[2-(3-cyanopropoxy)phenyl]-2,4-dioxobutanoic acid; Pyr) pyrogallol; CN-Pyr) cyanoacetylhydrazone 5-formylpyrogallol; DMSO) dimethylsulfoxide; HCV) hepatitis C virus; NTP) nucleoside triphosphate; RdRp) RNA-dependent RNA polymerase.

* To whom correspondence should be addressed.

single-subunit polymerases and catalyze the internucleotide binding [8-11]. Because under usual conditions of the enzymatic reaction, these ions interact with the pyrophosphate fragment of the attendant nucleoside triphosphate (NTP), such inhibitors are considered as mimetics of pyrophosphate [8, 9]. The chelation by DKA oxygen-containing groups of magnesium ions in the active site is thought to prevent the binding of the pyrophosphate group of the nucleotide substrate and, thus, formation of the phosphodiester bond, whereas the aromatic ring substituents (R) are essential for the specificity and efficiency of interaction with the enzyme [9]. However, it should be noted that some experimental findings and, first of all, the noncompetitive inhibition with respect to both NTP and RNA template, contradict this mechanism [6, 8]. Therefore, to establish the true mechanism of the inhibition, additional biochemical and structural studies are necessary.

Because the pyrogallol derivatives described earlier by us also include the corresponding oxygen-containing ligands (Fig. 1b) and reversibly inhibit HCV RdRp without competition with NTP [12], these compounds were expected to act similarly. This circumstance has determined our work.

MATERIALS AND METHODS

Chemicals. The reagents used were as follows: pyrogallol (Acros Organics, Belgium); 5-formylpyrogallol (Aldrich, USA); the *Escherichia coli* strain BL-2-CodonPlus® (DE3)-RIL (Stratagene, USA); Ni-NTA agarose (Novagen, USA); poly(U)-Sepharose CL-6B (Amersham, England); bactotryptone and yeast extract (Difco, USA); Tris and 2-mercaptoethanol (Merck, Germany); glycerol, dithiothreitol, imidazole, Triton X-100, Nonidet P-40, ammonium persulfate, phenylmethylsulfonyl fluoride (PMSF), and leupeptin (Sigma, USA); EDTA and pepstatin (Serva, Germany). Other reagents were of special or chemical purity qualification (Reakhim, Russia).

Synthesis of pyrogallol derivatives. The substituted pyrogallol derivatives **1-7** were prepared by one step, based on 5-formylpyrogallol and the corresponding amino compound (Scheme). The general procedure of the synthesis was as follows. To solution of 5-formylpyrogallol monohydrate (86 mg, 0.5 mmol) in 1 ml of ethanol, 1.2 equivalents of the mixture of the amino component and AcOH (30 mg, 0.5 mmol) were added. After incubation for 2-3 h at room temperature, the product was isolated by filtration or chromatography with the yield of 50-85%. The structure of the resulting compounds was confirmed by ^{1}H-NMR (DMSO-d6) and mass spectrometry (ESI MS) in some cases.

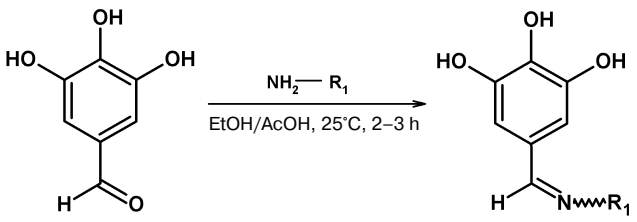

General scheme of synthesis of 5-substituted pyrogallol derivatives **1-7**

The data of NMR and ESI MS:

1) δ 9.20 (s, 2H, OH), 8.79 (s, 1H, OH), 8.26 (s, 1H, CH), 7.37 (t, J = 8.1 Hz, 2H, CH), 7.19 (t, J = 8.1 Hz, 3H, CH), 6.89 (s, 2H, CH);

2) (*cis*, *E*) δ 10.95 (s, 1H, NH), 9.08 (s, 2H, OH), 8.55 (s, 1H, OH), 7.70 (s, 1H, CH), 6.58 (s, 2H, CH), 2.15 (s, 3H, CH_3); (*trans*, *E*) δ 11.08 (s, 1H, NH), 9.08 (s, 2H, OH), 8.55 (s, 1H, OH), 7.84 (s, 1H, CH), 6.62 (s, 2H, CH), 1.90 (s, 3H, CH_3);

3) δ 9.07 (s, 2H, OH), 8.54 (s, 1H, OH), 7.91 (s, 1H, CH), 6.55 (s, 2H, CH), 3.80 (s, 3H, CH_3);

4) δ 8.90 (s, 2H, OH), 8.25 (s, 1H, OH), 7.44 (s, 1H, CH), 6.54 (s, 2H, CH), 3.73 (t, J = 4.7 Hz, 4H, CH_2), 2.99 (t, J = 4.7 Hz, 4H, CH_2);

5) δ 8.91 (s, 4H, OH), 8.27 (s, 2H, OH), 7.47 (s, 2H, CH), 6.56 (s, 4H, CH), 3.17 (s, 8H, CH_2);

6) (*cis*, *E*) δ 11.50 (s, 1H, NH), 9.12 (s, 2H, OH), 8.65 (s, 1H, OH), 7.72 (s, 1H, CH), 6.61 (s, 2H, CH), 4.11 (s, 2H, CH_2); (*trans*, *E*) δ 11.44 (s, 1H, NH), 9.14 (s, 2H, OH), 8.64 (s, 1H, OH), 7.86 (s, 1H, CH), 6.66 (s, 2H, CH), 3.74 (s, 2H, CH_2); ESI MS: m/e $C_{10}H_9N_3O_4$ 236.1 $[M + H]^+$;

7) (*cis*, *E*) δ 7.65 (s, 1H, CH), 6.56 (s, 2H, CH), 2.99 (s, 2H, CH_2); (*trans*, *E*) δ 12.93 (s, 1H, NH), 9.06 (s, 1H, OH), 7.84 (s, 1H, CH), 6.64 (s, 2H, CH), 2.81 (s, 2H, CH_2); ESI MS: m/e $C_{10}H_9N_2O_6K$ 293.1 $[M + H]^+$.

Inhibition of HCV RdRp by pyrogallol derivatives. Isolation of HCV RdRp and determination of its activity were performed as described in our previous work [12]. Values of IC_{50} for the inhibitors were determined as described in [12] in the concentration range from 0.3 μM to 1 mM. The inhibitors were introduced into the reaction medium after preincubation with UTP. The error in the IC_{50} determination in four parallel experiments was 10-20%.

Molecular modeling and docking were performed using an Indigo 2 workstation (Silicon Graphics) using Turbo Frodo [13] and Molscript [14] programs.

RESULTS AND DISCUSSION

In this work, we wanted to find out why pyrophosphate mimetics inhibit RdRp in a noncompetitive manner with regard to NTP. We supposed that this should be

associated with specific features of the polymerase reaction. It is known that the open conformation of DNA and RNA single-subunit polymerases transforms to the closed one during the one link elongation cycle of the polynucleotide chain, and these conformations correspond to the catalytically inactive and active state of the complex. It is generally thought that in the open conformation NTP is bound in the so-called pre-insertion site (the primary binding site) located in the NTP entrance channel at some distance from the catalytic site. The subsequent transition to the closed conformation is accompanied by the relocation of the NTP into the insertion site (the proper catalytic site) [15]. To realize the next cycle of the nucleotide binding, the enzyme has to come back to the open state.

The kinetics and thermodynamics of the reaction catalyzed by HCV RdRp have not been analyzed in detail. However, such an analysis was performed for the closely related polymerase of the poliovirus 3D, and there are convincing reasons to suggest a similar action mechanism for the majority of RNA-dependent RNA polymerases of animal viruses [16, 17]. Thus, during the elongation cycle, two stages are partially rate-limiting—the transition from the open conformation to the closed one previously to the phosphoryl transfer and the transfer itself onto the 3′-end of the growing polynucleotide chain [16, 17]. Obviously, pyrophosphate mimetics can mainly influence just these rate-limiting stages. Therefore, two explanations can be given for the mechanism of the observed noncompetitive inhibition: i) the inhibitor is bound in the catalytic region of the open complex and thus prevents the formation of the productive closed complex, and ii) the inhibitor is bound in the productive closed complex and prevents the phosphoryl transfer.

The noncompetitive inhibition suggests a synchronous and independent binding of the substrate and inhibitor, without overlapping of their binding sites. The structural analysis of HCV RdRp shows that the "fingers" subdomain of the enzyme has a manifold lower mobility than other single-subunit polymerases. Therefore, the primary binding site of NTP formed by this subdomain is located nearer to the proper catalytic site [5, 18]. Thus, the concurrent binding in the active site of the substrate and inhibitor in the open complex is unlikely because of steric obstacles. Moreover, the concurrent and independent entrance of the substrate and inhibitor into the region of the enzyme catalytic site (required by the noncompetitive mechanism) is fundamentally impossible, because the same NTP entrance channel has to be used.

We think that a successive development of the events is more likely: the inhibitor penetrates to the catalytic site through the vacant NTP entrance channel and binds with the catalytic complex just at the phosphoryl transfer stage. The interaction strength is ensured by the synchronous chelation of two magnesium ions. The formation of such a triple complex can result in "arresting" the enzyme at the phosphoryl transfer stage due to changes in the NTP coordination. The possibility of such a noncompetitive mechanism of inhibition depends on specific features of the three-dimensional structure of the catalytic complex and, first of all, the distance between the magnesium ions and their availability for the additional chelation by the inhibitor molecule.

Molecular modeling and docking. Because the crystalline structure of the elongation complex of HCV RdRp is not yet determined, the inhibitor can be docked into the active site only by means of molecular modeling. For this purpose, the three-dimensional structure of the HCV RdRp complex with UTP [5] was superposed with the complete initiating complex of the bacteriophage ϕ6 RNA-dependent RNA polymerase (RdRp ϕ6), which is a structural analog of HCV RdRp [19]. As the base element for the superposition, the catalytic loop with two of three aspartate catalytic residues (D318-D319 and D453-D454, respectively) was chosen. As a result, the three-dimensional model of the HCV RdRp active site was obtained containing the attendant GTP and two catalytic Mg^{2+} ions from the RdRp ϕ6 initiating complex.

Pyrogallol and DKA were chosen as starting compounds for the docking near the NTP binding site. It was found that the conformation of the substrate triphosphate residue and the spatial location of the two Mg^{2+} ions made possible their additional chelation by three oxygen atoms of each inhibitor. In both cases, the aromatic rings were located in the same plane and occupied the vacant space in the NTP substrate entrance tunnel between the catalytic site and the site of the NTP primary binding. According to this model, the primer and template cannot cause steric difficulties for binding both inhibitors, and this is indirectly confirmed by the noncompetitive manner of the inhibition observed in the literature [6, 8].

The next stage of the docking was performed using the earlier described *o*-substituted DKA derivative, 4-[2-(3-cyanopropoxy)phenyl]-2,4-dioxobutanoic acid (CN-DKA), which displayed an about 16-fold higher affinity for RdRp than the unsubstituted DKA [11] (Fig. 2a). Figure 3a shows the results of this compound docking into the HCV RdRp elongation complex modeled by us. The substituent orientation is shown according to data of the work [8] completely correlating with our model. It is supposed that the affinity of CN-DKA to the enzyme can increase due to formation of a hydrogen bond between the inhibitor cyano group and the conformationally mobile residue Arg222.

For docking pyrogallol derivatives, the molecule of cyanoacetyl hydrazone 5-formylpyrogallol (CN-Pyr) was chosen (Fig. 2b) as an analog of CN-DKA. The superposition of the structures of these two compounds indicated (Fig. 2c) that the distance between their cyano groups was no more than 2.5 Å. The docking of the CN-Pyr *cis*-conformation (which is prevalent in solution) revealed that the aromatic ring and side chain of this compound were

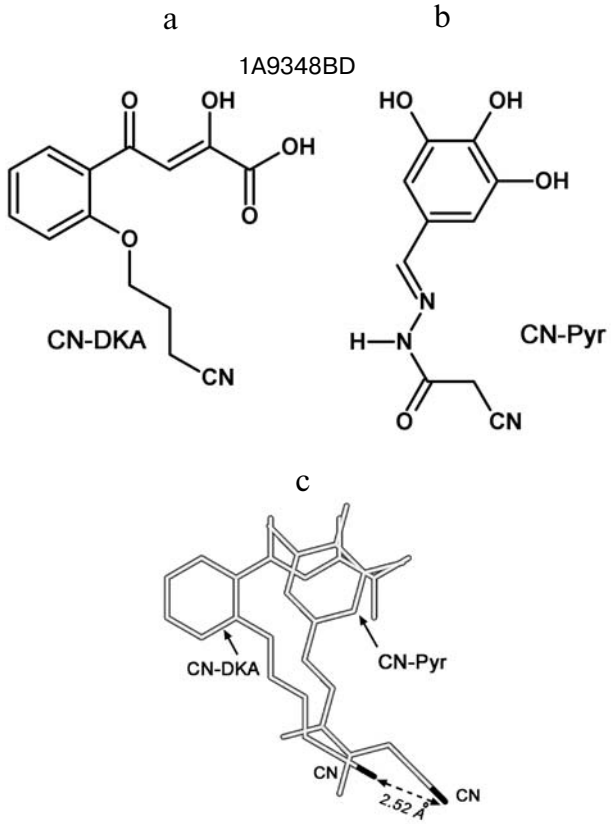

Fig. 2. Structures of CN-DKA (a) [5] and CN-Pyr (b). Superposition of these structures in the optimal conformations (c).

coplanar with the corresponding fragments of CN-DKA in the active conformation [8], and the terminal cyano group could interact with the same Arg222 residue of the enzyme (Fig. 3b).

Synthesis of 5-substituted pyrogallol derivatives. With the modeling results in mind, we synthesized a number of azomethine derivatives of pyrogallol, including CN-Pyr, based on 5-formylpyrogallol and the corresponding amino compound (see Scheme). Due to high yield and availability of the original reagents, it was possible to synthesize various compounds (table). In the case of O-methyloxime **3**, the product was one of two putative *E/Z* isomers. As expected, all other compounds were present in the solution only in the *E*-form. In the case of acylhydrazones **2**, **6** (CN-Pyr), and **7**, an additional *cis/trans* conformational equilibrium of the carbonyl substituent was revealed by NMR at the amide bond in the ratios of 61/39, 71/29, and 21/79, respectively (Fig. 4a) [20]. The prevalent *trans*-conformation of compound **7** was a result of formation of an intramolecular hydrogen bond (Fig. 4b), which was confirmed by the about 1.5 ppm downfield shift of the NH signal in the NMR spectrum.

Inhibitory properties of pyrogallol derivatives. The produced pyrogallol derivatives in micromolar concentrations inhibited the HCV RdRp activity in a reversible and noncompetitive manner with respect to UTP (table), and this was in agreement with our results published earlier [12]. The partial or complete O-methylation of the pyrogallol residue in all compounds abolished the inhibi-

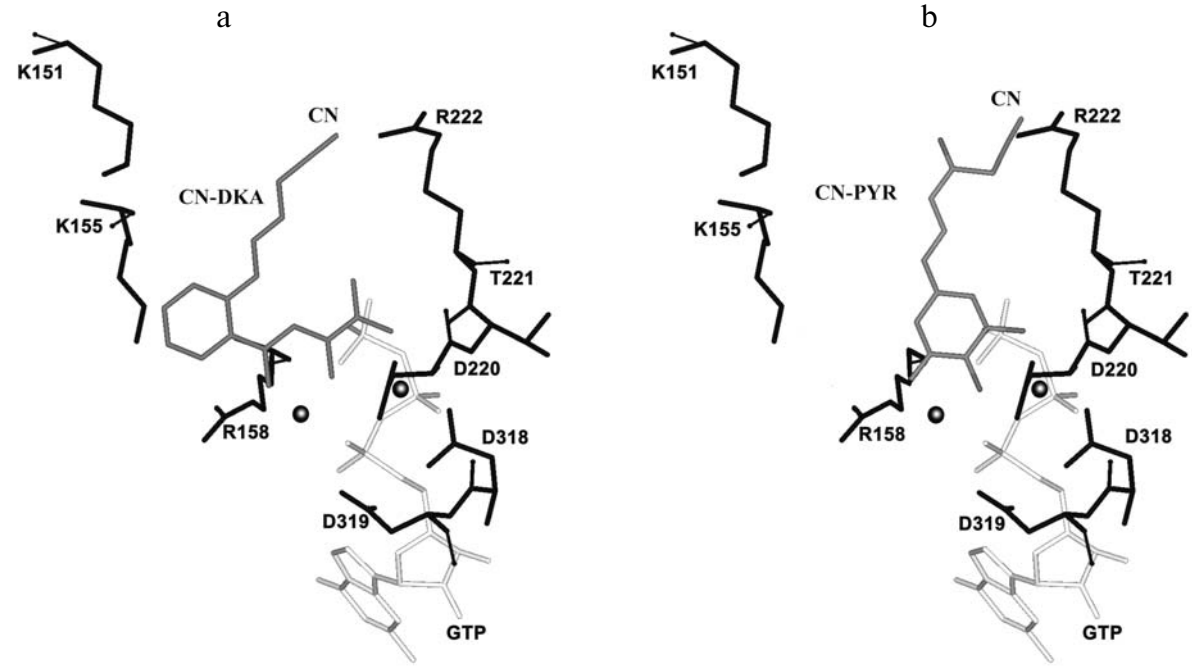

Fig. 3. Models of the CN-DKA (a) and CN-Pyr (b) binding in the active site of HCV RdRp. The enzyme amino acid residues are shown in black, the inhibitor molecules are gray, GTP is white, and Mg^{2+} ions are shown by circles.

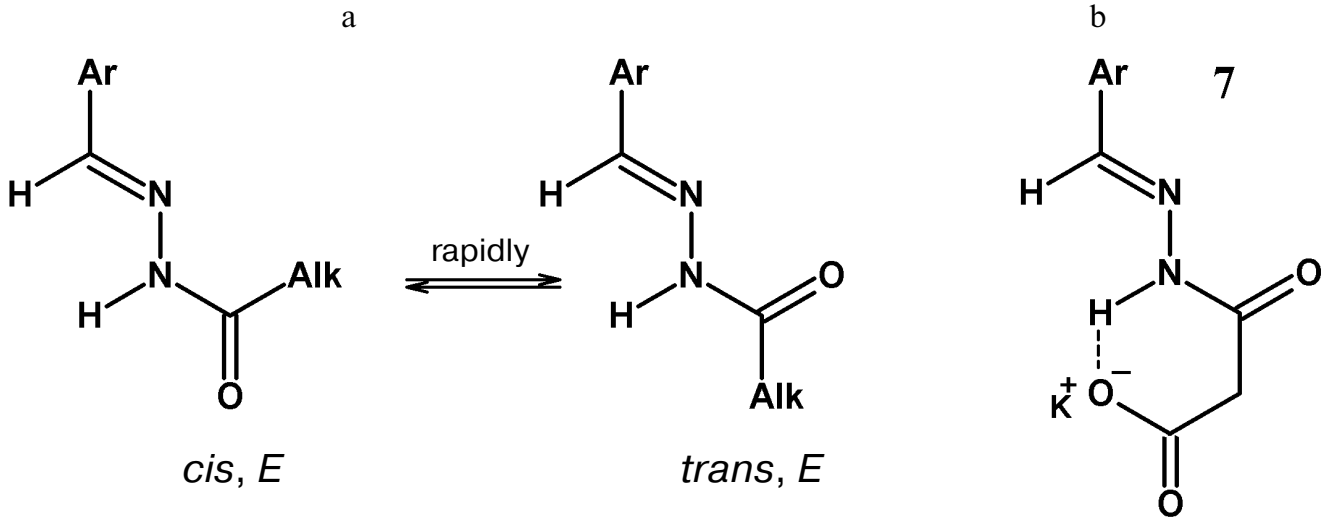

Fig. 4. The *cis/trans* equilibrium of acylhydrazones (a); compound **7** in the dominant *trans*, *E*-conformation (b).

tion (data not presented). A similar result was also observed earlier in the case of DKA methyl ester [8].

As differentiated from pyrogallol, 5-formylpyrogallol virtually did not inhibit the enzyme (table). In particular, this could be caused by the negative mesomeric (−M) effect of the formyl group. In the table, the compounds **1-5** prepared by us are arranged in order of the gradual decrease (−M) in the influence of the substituent R_1, assessed by the averaged value of the chemical shift of three phenolic protons of pyrogallol (Σσ(HO)/3). The calculated values (−M) of the influence were in a good correlation with the experimental values of IC_{50}. Note that compound **5** containing two pyrogallol residues inhibited the enzyme twofold stronger than compound **4**, possibly, simply due to doubling of the effective concentration of the pyrogallol residue. Thus, the piperazine and morpholine residues did not significantly contribute to the interaction with the enzyme.

Cyanoacetylhydrazone **6** (CN-Pyr) and carboxyacetylhydrazone **7** sharply increased the inhibition as compared to acetylhydrazone **2**. The affinity of CN-Pyr for RdRp increased about 13-fold as compared to **2** (table), or 18-fold on recalculation to the *cis*-conformer concentration (71% in solution). Thus, the introduction of the cyano group into the acyl residue of the inhibitor performed in accordance with the superposition and

Inhibition of HCV RdRp activity by pyrogallol derivatives

Compound	R_1	IC_{50}, μM	Σσ(HO)/3, ppm*
Pyrogallol		10	8.49
5-Formylpyrogallol		1000	9.40
1	Ph-	500	9.06
2	Ac-NH-	90	8.90
3	Me-O-	12	8.89
4		10	8.68
5		5.0	8.70
6	$NC-CH_2-CO-NH-$	7.0	8.96
7	$KO_2C-CH_2-CO-NH-$	3.0	—

* Averaged value of ^1H chemical shift of pyrogallol OH groups in DMSO.

docking results gave the expected increase in inhibition. This is a rather convincing argument in favor of our model of the action of pyrogallol derivatives and DKA on HCV RdRp.

The substitution of the neutral cyano group by the negatively charged carboxy group in compound **7** (table) additionally increased the inhibition 2.3-fold, or 7.9-fold on recalculation to the *cis*-conformer (21% in solution). This seems to indirectly indicate an additional electrostatic interaction with the positively charged residue Arg222.

At present, we have substituted R222V in the amino acid sequence of HCV RdRp. Studies on properties of the mutant enzyme seems to be promising for obtaining additional arguments in favor or against the inhibition mechanism supposed by us.

The present study is the first attempt to explain a sophisticated mechanism of the HCV RdRp inhibition by pyrophosphate mimetics. We think that the inhibition occurs at the stage of the phosphoryl transfer as a result of chelation of both catalytic Mg^{2+} ions of the catalytic site. The supposed mechanism is confirmed by the data of kinetics, molecular modeling, docking, and optimization of the inhibitor structures. The putative role of the Arg222 residue in the inhibition is now under study.

This work was supported by the Russian Foundation for Basic Research (project Nos. 01-04-48560 and 03-04-49154) and the Russian Academy of Sciences Presidium Program on Molecular and Cellular Biology.

REFERENCES

1. Rosen, H. R., and Gretch, D. R. (1999) *Mol. Med. Today*, **5**, 393-399.
2. *Report of a WHO Consultation Organized in Collaboration with the Viral Hepatitis Prevention Board*, Antwerp, Belgium (1999) *J. Viral. Hepat.*, **6**, 35-47.
3. Seeff, L. B., and Hoofnagle, J. H. (2003) *Clin. Liver Dis.*, **7**, 261-287.
4. Davis, G. L., Esteban-Mur, R., Rustgi, V., Hoefs, J., Gordon, S. C., Trepo, C., Shiffman, M. L., Zeuzem, S., Craxi, A., Ling, M. H., and Albrecht, J. (1998) *N. Engl. J. Med.*, **339**, 1493-1499.
5. Bressanelli, S., Tomei, L., Rey, F. A., and de Francesco, R. (2002) *J. Virol.*, **76**, 3482-3492.
6. De Francesco, R., Tomei, L., Altamura, S., Summa, V., and Migliaccio, G. (2003) *Antiviral Res.*, **58**, 1-16.
7. Gordon, C. P., and Keller, P. A. (2005) *J. Med. Chem.*, **48**, 1-20.
8. Summa, V., Petrocchi, A., Pace, P., Matassa, V. G., de Francesco, R., Altamura, S., Tomei, L., Koch, U., and Neuner, P. (2004) *J. Med. Chem.*, **47**, 14-17.
9. Summa, V., Petrocchi, A., Matassa, V. G., Taliani, M., Laufer, R., de Francesco, R., Altamura, S., and Pace, P. (2004) *J. Med. Chem.*, **47**, 5336-5339.
10. Grobler, J. A., Stillmock, K., Hu, B., Witmer, M., Felock, P., Espeseth, A. S., Wolfe, A., Egberston, M., Bourgeois, M., Melamed, J., Wai, J. S., Young, S., Vacca, J., and Hazuda, D. J. (2004) *Proc. Natl. Acad. Sci. USA*, **99**, 6661-6666.
11. Maurin, C., Bailly, F., Buisine, E., Vezin, H., Mbemba, G., Mouscadet, J. F., and Cotelle, P. (2004) *J. Med. Chem.*, **47**, 5583-5586.
12. Ivanov, A. V., Kozlov, M. V., Kuzyakin, A. O., Kostyuk, D. A., Tunitskaya, V. L., and Kochetkov, S. N. (2004) *Biochemistry (Moscow)*, **69**, 782-788.
13. Roussel, A., and Cambillau, C. (1991) *Silicon Graphics Geometry Partners Directory*, Mountain View, CA, USA, Silicon Graphics, p. 81.
14. Kraulis, P. J. (1991) *J. Appl. Crystallogr.*, **24**, 946-950.
15. Temyakov, D., Patlan, V., Anikin, M., McAllister, W. T., Yokoyama, S., and Vassylyev, D. G. (2004) *Cell*, **116**, 381-391.
16. Arnold, J. J., and Cameron, C. E. (2004) *Biochemistry*, **43**, 5126-5137.
17. Castro, C., Arnold, J. J., and Cameron, C. E. (2005) *Virus Res.*, **107**, 141-149.
18. O'Farell, D., Trowbridge, R., Rowlands, D., and Jager, J. (2003) *J. Mol. Biol.*, **326**, 1025-1035.
19. Butcher, S. J., Grimes, J. M., Makeyev, E. V., Bamford, D. H., and Stuart, D. I. (2001) *Nature*, **410**, 235-240.
20. Palla, G., Predieri, G., Domiano, P., Vignali, C., and Turner, W. (1986) *Tetrahedron*, **42**, 3649-3654.